HHS Public Access

Author manuscript

Neuroimage. Author manuscript; available in PMC 2017 November 15.

Published in final edited form as:

Neuroimage. 2016 November 15; 142: 474–482. doi:10.1016/j.neuroimage.2016.08.007.

CALIBRATED BOLD FMRI WITH AN OPTIMIZED ASL-BOLD DUAL-ACQUISITION SEQUENCE

María A. Fernández-Seara[1], **Zachary B. Rodgers**[2], **Erin K. Englund**[2], and **Felix W. Wehrli**[2]

[1]Department of Radiology, University of Navarra Hospital, Pamplona, Spain

[2]Laboratory for Structural, Physiologic and Functional Imaging, Department of Radiology, University of Pennsylvania Medical Center, Philadelphia, Pennsylvania, USA

Abstract

Calibrated fMRI techniques estimate task-induced changes in the cerebral metabolic rate of oxygen ($CMRO_2$) based on simultaneous measurements of cerebral blood flow (CBF) and blood-oxygen- level-dependent (BOLD) signal changes evoked by stimulation. To determine the calibration factor M (corresponding to the maximum possible BOLD signal increase), BOLD signal and CBF are measured in response to a gas breathing challenge (usually CO_2 or O_2). Here we describe an ASL dual-acquisition sequence that combines a background-suppressed 3D-GRASE readout with 2D multi-slice EPI. The concatenation of these two imaging sequences allowed separate optimization of the acquisition for CBF and BOLD data. The dual-acquisition sequence was validated by comparison to an ASL sequence with a dual-echo EPI readout, using a visual fMRI paradigm. Results showed a 3-fold increase in temporal signal-to-noise ratio (tSNR) of the ASL time-series data while BOLD tSNR was similar to that obtained with the dual-echo sequence. The longer TR of the proposed dual-acquisition sequence, however, resulted in slightly lower T-scores (by 30%) in the BOLD activation maps. Further, the potential of the dual-acquisition sequence for M-mapping on the basis of a hypercapnia gas breathing challenge and for quantification of $CMRO_2$ changes in response to a motor activation task was assessed. In five subjects, an average gray matter M-value of 8.71±1.03 and fractional changes of $CMRO_2$ of 12.5±5% were found. The new sequence remedies the deficiencies of prior combined BOLD-ASL acquisition strategies by substantially enhancing perfusion tSNR, which is essential for accurate BOLD calibration.

Keywords

arterial spin labeling; calibrated BOLD; $CMRO_2$ quantification; background suppression; 3D GRASE; dual-echo EPI

Corresponding author: María A. Fernández-Seara, Department of Radiology, University of Navarra Hospital, Pio XII, 36, 31008 Pamplona, Spain, Voice: ++ 34 948 255400, mfseara@unav.es.

DISCLOSURE/CONFLIC OF INTEREST

The authors declare no conflict of interest.

1. INTRODUCTION

Functional MRI (fMRI) based on blood oxygen level dependent (BOLD) contrast offers an indirect measurement of neural activity changes. BOLD contrast originates from the increase in blood water effective transverse relaxation time, T_2*, induced by a decrease in the concentration of deoxyhemoglobin (dHb) in the venous vasculature during neural activation. This decrease in dHb concentration ([dHb]) arises from a local increase in cerebral blood flow (CBF), which overcompensates the rise in the cerebral metabolic rate of oxygen consumption ($CMRO_2$) (McIntyre, et al., 2003). Thus, BOLD contrast is a complex function of the underlying changes in several physiological parameters. Moreover, the amplitude of the BOLD response depends as well on [dHb], the concentration of deoxyhemoglobin in the voxel during the baseline state, which is determined by hematocrit, oxygen extraction fraction and cerebral blood volume (CBV) (Blockley, et al., 2013). The interplay of these different variables, which cannot be derived from a simple fMRI experiment, precludes quantitative interpretation of BOLD signal changes.

Calibrated fMRI, proposed by Davis et al. in 1998, offers a quantitative alternative to BOLD by permitting computation of $CMRO_2$ changes, a direct consequence of the energy expenditure associated to brain activation (Davis, et al., 1998). The Davis model relates BOLD signal changes evoked by stimulation to $CMRO_2$ and CBF, via the following expression:

$$\frac{\Delta \mathrm{BOLD}}{\mathrm{BOLD}_0} = M\left(1-\left(\frac{CMRO_2}{CMRO_2\big|_0}\right)^{\beta}\left(\frac{CBF}{CBF_0}\right)^{\alpha-\beta}\right) \quad [1]$$

where the subscript 0 indicates the baseline state, α characterizes the power law relationship between CBV and CBF (Grubb, et al., 1974), β defines the supralinear effect of [dHb] on T_2* changes and M is the BOLD calibration factor, given by:

$$M = TE \cdot A \cdot CBV_{V_0} \cdot [dHB]^{\beta}_{V_0} \quad [2]$$

where TE is the echo time, A is a scaling factor that depends on several parameters including vessel geometry, magnetic field strength and the susceptibility difference between blood and tissue and the subscript V_0 refers to the venous blood compartment during baseline.

Calibrated fMRI techniques require measurement of CBF changes, directly obtainable using arterial spin labeling (ASL) perfusion MRI, and BOLD changes, combined with a calibration experiment aimed at estimating the baseline condition. The calibration factor M, corresponding to the maximum possible BOLD signal increase (i.e. the signal increase that could be achieved with complete washout of dHb induced by a CBF increase without associated metabolic changes), is estimated using blood gas manipulation techniques, most often involving CO_2 or O_2 gas mixture breathing. Assuming that hypercapnic gas mixture

breathing does not induce changes in $CMRO_2$ (Jain, et al., 2011), M can be quantified from the measurement of BOLD and CBF changes relative to baseline, via the following expression:

$$M = \left(\frac{\Delta \mathrm{BOLD}}{\mathrm{BOLD}_0}\right)\left[1 - \left(\frac{CBF}{CBF_0}\right)^{(\alpha-\beta)}\right]^{-1} \quad [3]$$

However, this measurement is highly sensitive to ASL noise, due to the large exponent on the relative CBF changes present in the equation.

ASL is intrinsically a low signal-to-noise (SNR) technique due to the small fraction of arterial blood to tissue in the human brain (1–2%) (Liu and Brown, 2007) and to the relatively rapid decay rate of the label via T_1 relaxation during the arterial transit time. Furthermore, the ASL time series contains fluctuations from thermal and physiological noise sources. At high field strength and for the large voxel sizes typically necessary in ASL acquisitions, the contribution of physiological noise dominates the temporal SNR (tSNR) of the ASL time series. Background suppression (BS) of the static tissue signal is an effective technique to reduce motion artifacts and physiological noise (which scales with signal strength) and thus it has been shown to greatly improve the sensitivity of ASL (Garcia, et al., 2005; Ye, et al., 2000; Vidorreta, et al., 2013). BS is implemented by introducing several inversion pulses applied during the post-labeling delay, timed to achieve a target signal suppression level at the time of signal readout. Thus BS is optimally combined with 3D acquisitions because the entire imaging volume is excited at a single time point (Gunther, et al., 2005). Implementation of BS in 2D multi-slice acquisitions is hampered by the different slice acquisition times, which result in a variable degree of BS depending on the slice acquisition order.

Simultaneous CBF and BOLD data, as preferred for calibrated fMRI, can be achieved with a single-echo acquisition, however, in this approach both contrasts are compromised by the choice of TE, since for ASL the shortest possible TE should be used, while for BOLD TE should be on the order of T_2* (around 30 ms at 3T). Thus, more recently, there has been focus on ASL sequences with dual-echo (DE) readouts, generally DE 2D EPI (Liu, et al., 2002; Woolrich, et al., 2006), in which the first echo is used to obtained perfusion-weighted images by subtraction of label and control acquisitions, while the BOLD data is extracted from the second echo images. Here, background suppression is not desired as it would unduly attenuate the BOLD signal extracted from the second-echo images. One possible compromise consists of partially suppressing the static tissue signal in DE-EPI, which has been shown to increase the CBF sensitivity while only slightly decreasing the BOLD sensitivity (Ghariq, et al., 2014).

An alternative strategy to single-excitation approaches is a dual excitation sequence, essentially a concatenation of two imaging sequences, which has previously been proposed by several authors (Kastrup, et al., 2002; Schmithorst, et al., 2014; St Lawrence, et al., 2005; Stefanovic, et al., 2006; Wesolowski, et al., 2009). The benefit of this approach is that acquisition parameters can be separately optimized for each excitation. However, in all

previous studies 2D multislice readouts were employed for both acquisitions. Although two of these studies implemented BS in the ASL readouts (St Lawrence, et al., 2005; Wesolowski, et al., 2009), as mentioned, obtaining homogeneous BS in 2D multi-slice acquisitions is not possible.

The goal of this study was to design and implement an ASL dual-excitation/dual-acquisition sequence, henceforth referred to as dual-acquisition (DA) sequence, for simultaneous measurement of BOLD and CBF, by means of a background-suppressed 3D readout optimized for ASL, followed by a 2D EPI readout for acquisition of BOLD data, after a time delay to allow for signal recovery. It was hypothesized that this approach would provide optimal contrast-to-noise for both ASL and BOLD, thus improving the fidelity of derived BOLD calibration M-maps and $CMRO_2$ mapping. The performance of the sequence was evaluated in comparison to an ASL sequence with DE-EPI readout in an fMRI experiment with a visual activation paradigm. Finally its potential for M-mapping and quantification of $CMRO_2$ changes was assessed in response to a motor activation task.

2. MATERIALS AND METHODS

2.1 ASL-BOLD dual acquisition pulse sequence

The DA sequence (Fig. 1) consisted of a pseudo-continuous ASL (PCASL) module with a background-suppressed single-shot 3D-GRASE readout for acquisition of ASL images (Fernandez-Seara, et al., 2008; Gunther, et al., 2005) and multi-slice 2D-EPI for acquisition of BOLD images. Both readouts imaged the same volume and were separated by a delay of 1.3s to allow for recovery of the longitudinal magnetization. For labeling the PCASL pulse train consisted of 1520 selective radio-frequency (RF) pulses (Hanning window, peak B_1 average = 1.8 μT, duration = 500 μs, spacing = 500 μs, G average = 1 mT/m, G maximum / G average = 8) with a labeling duration of 1520 ms and post-labeling delay (PLD) of 1500 ms. For the control cycle, the RF phase was alternated between 0 and 180°. The gradient waveforms were identical for label and control acquisitions. The inversion plane was offset 8 cm from the center of the imaging volume in the infero-superior direction. For BS, the PCASL pulse train was preceded by 4 presaturation pulses played at the start of the repetition time and a slice-selective Frequency Offset Corrected Inversion (FOCI) pulse (Ordidge, et al., 1996), and followed by two non-selective hyperbolic secant inversion pulses, which were played out during the PLD. The inversion times were optimized to suppress the static tissue signal to 10% of its equilibrium value at the start of the 3D-GRASE readout for a range of T_1 values from 700 to 4500 ms (Vidorreta, et al., 2013).

2.2 Simulations

In order to evaluate the effect of the dual excitation on the signal intensity, the evolution of the longitudinal magnetization over the repetition time was simulated using analytical solutions of the Bloch equations for gray and white matter and CSF assuming T_1 values at 3T of 1300 ms, 800 ms and 4000 ms, respectively (Clare and Jezzard, 2001).

2.3 Experiments

Two sets of experiments were carried out. In the first, the performance of the DA sequence was compared to a PCASL DE-EPI sequence during a visual stimulation paradigm. In the second, the DA sequence was used in combination with a gas breathing challenge to obtain calibration factor M-maps and subsequently task-induced $CMRO_2$ changes during a motor activation paradigm.

Studies were performed on a 3T Trio TIM (Siemens AG, Erlangen, Germany) using a 32-channel head array. All subjects signed a written informed consent, following an Institutional Review Board approved protocol and were instructed to remain still with eyes open during the scanning session. Both sets of experiments included the acquisition of T_1-weighted anatomical images obtained with an MPRAGE sequence (Mugler and Brookeman, 1990), with the following imaging parameters: resolution = 1 mm isotropic, FOV = 192×256×160 mm^3, matrix = 192×256×160, TR/TE/TI = 1620/3.09/950 ms, flip angle = 15°.

Data analysis was performed using SPM (Version 8, Wellcome Trust Center for Neuroimaging, University College London, UK) and custom scripts in MATLAB (Mathworks, MA, USA).

2.4 Comparison between the dual acquisition sequence and dual echo EPI

Ten healthy volunteers (mean age ± standard deviation = 23.3 ± 4.8 years, 4 females) participated in the study.

2.4.1. Scan protocol—Subjects were scanned with both sequences in the same scanning session, in counter-balanced order, during a visual stimulation paradigm described below. The PCASL parameters were identical for the two sequences. Both sequences imaged the same volume. The imaging parameters of the DA sequence were: TE (GRASE/EPI) = 28.9 / 30 ms, TR = 6 s, FOV = 250 × 218 mm^2, in-plane resolution = 4 × 4 mm^2, matrix size = 64 × 56, BW = 2790 Hz/pixel, 16 axial slices, slice thickness = 6 mm. Additional 3D GRASE parameters were: 16 nominal partitions with 33% oversampling, 5/8 partial Fourier, measured partitions = 14, gradient-echo spacing = 0.4 ms (with ramp sampling), spin-echo spacing = 28.9 ms, total read-out time = 420 ms. The total read-out period for the 2D EPI part of the sequence was 730 ms. The imaging parameters for the DE-EPI readout were: TE1 = 10 ms, TE2 = 30 ms, TR = 4 s, FOV = 250 × 218 mm^2, in-plane resolution = 4×4 mm^2, matrix size = 64 × 56, BW = 2790 Hz/pixel, 16 axial slices, slice thickness = 6mm, GRAPPA acceleration factor = 2, total read-out time = 812 ms. A summary of sequence parameters are given in Table 1.

2.4.2. Visual stimulation paradigm—The stimulation paradigm consisted of three blocks of rest alternated with three blocks of visual stimulation, of 2 minutes duration per block. During rest, the subjects were presented with a gray cross on a white screen. The visual stimulus was a black and white checkerboard flashing at 8 Hz with a gray cross located at its center. Subjects were instructed to keep their eyes focused on the gray cross at all times.

2.4.3. Data pre-processing—The four series of images (ASL and BOLD from the DA sequence and ASL and BOLD from the DE-EPI sequence) were separately realigned to the first image in the series and coregistered to the anatomical image. ASL images were sinc-subtracted to obtain perfusion-weighted images without BOLD contamination (Aguirre, et al., 2002). Mean CBF maps were computed from the perfusion-weighted images acquired during the rest periods. Details of these calculations and their results are presented in Supplementary Material. The anatomical images were normalized to the Montreal Neurological Institute standard template brain and the resulting normalization parameters were used to compute normalized BOLD and perfusion-weighted images, which were re-sliced to an isotropic voxel size of 2 mm and smoothed using a 6 mm full-width at half-maximum isotropic Gaussian kernel.

2.4.4. Task activation data analysis—Voxel-wise analyses were carried out to identify voxels activated by visual stimulation. BOLD images obtained during the activation paradigm were entered into a general lineal model (GLM) with two conditions (rest and task). The model involved a regressor to account for the ASL effect (i.e. image being acquired during control or label conditions) and a linear drift term. A high-pass filter with a cutoff value of 512 s was included and serial correlations were accounted for using an autoregressive AR(1) model. Perfusion-weighted images were analyzed analogously, excluding the regressors and the temporal autocorrelation model. Contrast images comparing task and rest were obtained for each subject and entered into a second-level analysis.

For each subject, a mask was generated from the normalized BOLD images using an intensity threshold. A group mask was then computed as the intersection of all the individual subject masks and used in the second level analyses to remove out-of-brain voxels.

Activation group T-maps were obtained using a one-sample T-test and thresholded at a cluster level p-value of 0.05 (family-wise error corrected) after a cluster defining threshold of $p<0.001$. Two activation group maps were obtained in this manner (BOLD and perfusion) for each of the two datasets obtained with the DE-EPI and DA sequences.

Activated regions within each map were extracted as regions of interest (ROI) using Marsbar in SPM (Bret, et al., 2002). An ROI including the area of activation common to the four group maps was created as the intersection of the activated clusters. This ROI was used to extract signal time courses from each dataset and subject. To characterize the sensitivity of the functional data, the following parameters were extracted from these time courses: tSNR, relative signal change due to activation and contrast-to-noise ratio (CNR) of the signal. tSNR was computed as the mean of the signal during the rest periods divided by its standard deviation across time. The relative signal change due to activation was calculated as the mean of the signal during the task periods minus the mean of the signal during the rest periods, divided by the mean of the signal during rest. CNR was computed as the difference in signal between activation and rest periods divided by the averaged standard deviation (i.e. the average of the signal standard deviations during rest and activation). For time courses extracted from BOLD data, the relative signal change due to activation and CNR were computed after correcting the time course for baseline drift. The baseline drift was assumed

to be linear and it was estimated using a first-degree polynomial to fit the signal points acquired during rest.

The same ROI, defined to extract signal time-courses, was used to compute mean T-statistics for each subject and dataset. In addition, to evaluate the spatial extent of the BOLD and perfusion activations, individual activation maps were thresholded at T = 2.6 ($p<0.005$, uncorrected) and the number of activated voxels within the visual cortex was computed. To that end, a visual cortex mask was previously defined as the sum of Brodmann areas (BA) 17 (primary visual cortex, V1), 18 (secondary visual cortex, V2) and 19 (associative visual cortex, V3, V4 and V5), extracted from the BA template provided with MRIcroN (Rorden, et al., 2007).

Statistical differences in the mean parameter values across sequences were evaluated using paired T-tests, applied separately to each data modality. Since 10 comparisons were performed, Bonferroni correction was applied to the p-values to assess significance. Finally, for each subject and data modality (BOLD and perfusion) the ratio of each parameter value obtained with the DA sequence to the same parameter value obtained with the DE-EPI sequence was calculated.

2.5. Estimation of $CMRO_2$ changes during task activation

Five healthy male volunteers (age = 34 ± 6 years) participated in this experiment.

2.5.1. Scan protocol—Functional data were obtained with the DA sequence, with the imaging parameters described above. First, data were continuously acquired throughout a gas mixture breathing protocol, during which room air was delivered for 5 minutes (baseline), followed by 5 minutes of hypercapnia (HC) consisting of subjects breathing a mixture of 5% CO_2 in room air, to end with 5 minutes of room air (recovery). During the HC period, the gas mixture was delivered using a two-way non-rebreathing T-valve (2700 Series, Hans Rudolph, Inc., Kansas City, MO, USA) attached to a 100 L Douglas bag. The HC experiment was followed by one run with a motor activation paradigm of 6 min duration, divided into 3 blocks of bilateral finger tapping alternated with 3 rest blocks of 1 min duration each.

2.5.2. Data pre-processing—ASL and BOLD images were separately pre-processed. BOLD images were realigned to the first image in the BOLD time-series and smoothed, using a 6-mm Gaussian kernel. ASL images were realigned to the first image in the ASL time-series, followed by subtraction of label and control to obtain perfusion-weighted images and smoothing.

T_1-weighted anatomical images were segmented to generate tissue probability maps. Subsequently, they were coregistered to the BOLD images and resliced to match the resolution of the BOLD images. A gray matter mask was then generated from the coregistered, resliced and smoothed gray matter probability map applying a threshold of 0.3.

A whole brain mask was generated from the BOLD images applying a threshold of 0.8 of the maximum signal intensity. A gray matter ROI was then defined as the intersection of the

gray matter mask obtained from the anatomical image with this whole brain mask, to exclude voxels of signal void in the BOLD images.

2.5.3. Gas manipulation data analysis—BOLD images obtained during gas manipulation were entered into a GLM with two conditions (room air and hypercapnia), excluding the first minute after each transition. The model involved a regressor to account for the ASL effect and a linear drift term. The regression coefficients were used to compute signal baseline level ($BOLD_0$) and signal change induced by HC (ΔBOLD). Perfusion-weighted images were entered into a similar GLM without regressors to compute the perfusion signal at baseline and during HC and HC-induced signal change. M-maps were calculated via Eq. 3, with $\alpha = 0.18$ (Grubb, et al., 1974) and $\beta = 1.5$ (Boxerman, et al., 1995). The gray matter ROI previously defined was used to compute mean gray matter signal change (BOLD and perfusion) induced by hypercapnia and the average gray matter M value.

2.5.4. Task activation data analysis—BOLD images obtained during the activation paradigm were entered into a GLM with two conditions (rest and task) and a regressor to model the ASL effect. Perfusion-weighted images were analyzed analogously, excluding the regressor. Contrast images comparing task and rest were obtained for each subject. Activated regions were identified using an uncorrected p-value of 0.005. ROIs were defined in the left and right motor cortex (MC), including voxels that appeared active in both analyses, and used to extract signal time-courses. Relative $CMRO_2$ maps were computed via Eq. 1.

3. RESULTS

3.1. Simulations

Fig. 2 shows the evolution of M_z (the longitudinal component of the magnetization vector) over the TR of the DA sequence, obtained by simulations. The timings of the BS pulses have been optimized to suppress the static tissue signal to 10% of its original value at the start of the 3D GRASE readout, as shown in the graph. The magnetization then relaxes towards its equilibrium value during the 1.3 s delay between the two readouts. During the 2D EPI readout, the gray matter M_z (blue line) will vary from 0.63 to 0.79 of its equilibrium value at the time of imaging for each slice, depending on slice position.

3.2. Comparison between the dual acquisition sequence and dual echo EPI

Whole-brain mean CBF values measured during rest with the DE-EPI and DA sequences were identical (details are included in Supplementary Material).

Fig. 3a shows the areas activated by visual stimulation obtained from the four datasets acquired in a representative subject. Fig. 3b illustrates the corresponding signal time-courses extracted from the group maps intersection ROI, as described in the methods section. Table 2a lists the signal parameters measured for each sequence and data modality. Table 2b shows the ratio of signal parameters between sequences for each data modality.

tSNR of the perfusion signal was significantly higher by a factor of 3 in the DA sequence compared to the DE-EPI sequence. However, the signal change due to activation was

significantly lower by 32%. As a result, the CNR was greater by 75% in the DA acquisition sequence. For the BOLD data, tSNR, signal change due to activation and CNR were slightly lower in the DA compared to the DE-EPI sequence, although the differences were not statistically significant. Similarly, perfusion mean T-scores were significantly higher by 65% in the DA sequence compared to the DE-EPI sequence, while BOLD mean T-scores were significantly lower by 27%. In addition the DA sequence also affected the spatial sensitivity of the BOLD and perfusion activations. On average, the individual areas of activation (thresholded at T=2.6, $p<0.005$ uncorrected) were significantly larger by a factor of 5 for perfusion data but were smaller by a factor of 1.2 for BOLD data (not significant), in comparison to the DE-EPI sequence. In summary, the DA sequence yielded significantly greater ASL tSNR, CNR, T-scores and spatial sensitivity, with only modest and mostly non-significant reductions in corresponding BOLD activation values.

3.3. Estimation of $CMRO_2$ changes during task activation

Fig. 4 shows the signal difference images and M-map, computed from the gas manipulation data, in a representative subject. BOLD and perfusion signal changes induced by hypercapnia in gray matter and M values are shown in Table 3. Fig. 5 (a–c) shows maps of signal change induced by bilateral finger tapping, revealing bilateral activation of the motor cortex (MC). Relative $CMRO_2$ time-courses in the activated regions are shown in Fig. 5d. Individual and group-averaged calibrated fMRI parameters, including mean M values for the left and right MC ROIs, as well as task-evoked signal changes are given in Table 3. Mean evoked $CMRO_2$ estimates found were 12 and 13 % for left and right MC, respectively. Assuming a resting state value for gray matter $CMRO_2$ of 146 μmol/100g/min (Bulte, et al., 2012), the observed fractional changes would correspond to absolute changes of 17 and 19 μmol O_2/100g/min.

4. DISCUSSION

In this work an improved method for simultaneous acquisition of CBF and BOLD data is presented for calibrated BOLD fMRI (Davis, et al., 1998). Calibration parameter maps have been obtained on the basis of a hypercapnia gas breathing challenge and used to estimate $CMRO_2$ changes induced by motor activation.

Currently, most works focusing on simultaneous acquisition of CBF and BOLD data for BOLD calibration employ an ASL sequence with dual-echo readout, in which the first echo is used to obtained perfusion-weighted images while the BOLD data is extracted from the second-echo images of longer TE (on the order of T2*) as a means to maximize BOLD contrast. Acquiring two echoes with the appropriate TEs is facilitated by the use of parallel imaging (GRAPPA or SENSE), or by using partial Fourier acquisitions, with both approaches entailing a signal-to-noise penalty. In distinction, in the present work ASL and BOLD data are collected from separate, successively applied excitations (referred to as dual-acquisition, DA). The benefit of this approach is that acquisition parameters can be separately optimized for each type of data modality. ASL data is acquired using a background-suppressed 3D-GRASE readout and BOLD data as a 2D EPI readout with appropriate TE, after a time delay to allow for recovery of the longitudinal magnetization.

The DA sequence was compared to a DE-EPI sequence with the same PCASL module. Results show a significant improvement in the tSNR (×3) of the perfusion time series (as illustrated in Fig. 3b). The higher tSNR is due to the effect of background suppression, which reduces physiological noise and motion artifacts. These findings are in excellent agreement with previous reports (Vidorreta, et al., 2013). In contrast, the perfusion signal change due to activation relative to baseline was somewhat lower (×0.68). The latter may be due to greater partial volume effects in the 3D GRASE images, relative to 2D EPI, resulting from point-spread function blurring in the slice-encoding direction, caused by T_2 decay of the signal during the single-shot readout (of 420 ms duration). This effect has been shown to reduce the gray-to-white matter CNR of the perfusion-weighted images (Fernandez-Seara, et al., 2005; Gunther, et al., 2005; Vidorreta, et al., 2013) and it could affect the spatial specificity of the perfusion activation clusters. As a result, the perfusion time series CNR increase (×1.75) was lower than the tSNR increase. In spite of this, activation maps obtained from the perfusion data yielded higher mean T-scores (×1.68) and greater number of activated voxels for a set significance threshold (×5.68). The increased size of the activated clusters obtained with the DA acquisition sequence could be partly due to partial volume effects in the 3D GRASE images, although these clusters are still smaller than those obtained from the BOLD data and therefore they are likely to reflect truly activated area.

In our implementation, the duration of the single-shot 3D GRASE readout was reduced by means of partial Fourier sampling in the slice-encoding direction. We note that the scan could be accelerated further by using parallel imaging techniques (thereby shortening the echo-train duration), which, in turn, would enhance the slice resolution, thus decreasing partial volume effects, albeit exacting an SNR penalty.

When comparing the BOLD data derived with both sequences, there were no significant differences in tSNR, signal change upon activation or CNR. The simulation of the time evolution of the longitudinal magnetization during the pulse sequence cycle of the DA sequence indicates reduced gray matter BOLD signal (by about 30%), with respect to a conventional BOLD sequence, and varying slightly with slice location. The predicted lower BOLD signal results from incomplete recovery of the longitudinal magnetization and it will depend on the delay time between the two successive acquisitions.

The implementation of the DE-EPI sequence used in this work employs GRAPPA with an acceleration factor of 2, to facilitate sampling of the two echoes at the appropriate TEs. There is an image SNR penalty associated with the acceleration factor and the coil geometry factor (g), which is given by $g\sqrt{2}$. The 32-channel Siemens head array has previously been reported to have an average g factor close to 1 for R=2 (Keil, et al., 2011), which means the image SNR of the BOLD images should be lower by a factor of $\sqrt{2} = 1.4$ with respect to non-accelerated acquisitions. Therefore, SNR of the BOLD images acquired with the two sequences (DE-EPI and DA) should be similar.

Measurements of image SNR have not been performed in the experimental data because when multi-channel array coils are used, these measurements are complex (Triantafyllou, et al., 2011). Instead, measurements of temporal SNR and CNR are reported since they are

more straightforward and these parameters are the most important metrics for sensitivity in an fMRI experiment.

Even though BOLD tSNR and CNR ratio between sequences were not different, the activation maps obtained from the BOLD data yielded significantly lower mean T-scores (×0.73) and a lower number of activated voxels for a set significance threshold (×0.81) in the DA sequence. This is a consequence of the reduced number of data points (n) in the time series acquired with the DA sequence, due to its longer TR. For the same CNR (also known as effect size) T-scores are directly proportional to √n. In the experimental data, the ratio $\sqrt{n}_{DA}/\sqrt{n}_{DE\text{-}EPI} = \sqrt{TR}_{DE\text{-}EPI}/\sqrt{TR}_{DA}$ was √(4/6) = 0.81. Shortening TR for the DA sequence would avoid this penalty, which could be achieved by accelerating the readouts, specially the 2D EPI readout (currently 730 ms). Another possibility would be to shorten the time delay between the two readouts. However, the effects of these modifications on the SNR metrics would have to be evaluated. A potentially promising approach would consist of a single-shot 3D GRASE readout for acquisition of BOLD data. However achieving T_2* weighting with GRASE is not straightforward. GRASE is based on multiple spin-echoes and as such the echo train must fulfill the Carr-Purcell Meiboom-Gill (CPMG) condition. Introducing the T_2* preparation violates the CPMG condition, which causes severe signal loss or blurring in regions of magnetic field inhomogeneities. Several strategies have been proposed to implement phase-insensitive T_2* prepared multiple spin-echo sequences (Alsop, 1997; Jovicich and Norris, 1999; Norris, et al., 1992), but they all sacrifice SNR. Nonetheless, it would be a worthwhile strategy to be considered in future work.

The potential of the DA sequence for M-mapping and quantification of relative $CMRO_2$ changes was evaluated in response to a motor activation task. Hypercapnia induced signal changes (BOLD and perfusion) in gray matter were within the range of those reported previously (Gauthier and Hoge, 2013). M-maps demonstrated the expected gray to white matter contrast (see Fig. 4f) and averaged gray matter M values were in good agreement with literature results using hypercapnia calibration (Kastrup, et al., 2002; Leontiev and Buxton, 2007).

Maps of signal change induced by bilateral finger tapping obtained by BOLD and perfusion showed clusters of bilateral activation in the primary motor cortex. In addition, the highest sensitivity of the BOLD data indicated activation of the supplementary motor area. BOLD and perfusion signal changes in the MC due to activation were lower than signal changes induced by HC, as expected. Maps of relative $CMRO_2$ changes also revealed two clusters of activation in the motor cortex, clearly visible above background. Average relative increases in $CMRO_2$ of 12 and 13% were computed for left and right MC respectively, in very good agreement with reported $CMRO_2$ changes measured in a similar motor task (Kastrup, et al., 2002), corresponding to absolute changes of 17 and 19 μmol O_2/100g/min.

The results from this work validate the DA acquisition technique for calibrated BOLD fMRI. The new sequence substantially improves perfusion tSNR, the limiting factor for accurate BOLD calibration, thus overcoming the deficits of previous approaches. Moreover, previous calibrated fMRI techniques, while able to produce M maps via signal averaging over multiple cycles at baseline and hypercapnia, are poorly suited for subsequent application to

measurement of $CMRO_2$ changes in response to a functional tasks (because of the low ASL tSNR, which requires the task blocks to be either very long, or repeated many times). However, this limitation can be overcome by the proposed DA method. Future work will aim to improve the current implementation. The ASL portion of the sequence would benefit from a shortening of the 3D GRASE readout to reduce point-spread function blurring, while achieving a shorter TR would improve sensitivity for both ASL and BOLD data. Toward this aim, different strategies should be evaluated, such as the use of parallel imaging techniques or the implementation of a single-shot 3D readout for BOLD data acquisition.

5. CONCLUSION

In summary, the dual-acquisition strategy for simultaneous BOLD and CBF acquisition presented in this work, consisting of concatenation of two separate, individually optimized sequences, greatly improves tSNR of the ASL data, while achieving similar BOLD tSNR, relative to the dual-echo sequence.

Supplementary Material

Refer to Web version on PubMed Central for supplementary material.

Acknowledgments

The authors are indebted to Dr. Benedikt Poser for providing the code of the dual-echo EPI sequence.

This work was supported by the Spanish Ministry of Economy and Competitiveness (RYC-2010-07161, SAF2014-56330-R) and by the National Institutes of Health (RO1 HLI22754).

REFERENCES

Aguirre GK, Detre JA, Zarahn E, Alsop DC. Experimental design and the relative sensitivity of BOLD and perfusion fMRI. Neuroimage. 2002; 15:488–500. [PubMed: 11848692]

Alsop DC. Phase insensitive preparation of single-shot RARE: application to diffusion imaging in humans. Magn Reson Med. 1997; 38:527–533. [PubMed: 9324317]

Blockley NP, Griffeth VE, Simon AB, Buxton RB. A review of calibrated blood oxygenation level-dependent (BOLD) methods for the measurement of task-induced changes in brain oxygen metabolism. NMR Biomed. 2013; 26:987–1003. [PubMed: 22945365]

Boxerman JL, Hamberg LM, Rosen BR, Weisskoff RM. MR contrast due to intravascular magnetic susceptibility perturbations. Magn Reson Med. 1995; 34:555–566. [PubMed: 8524024]

Bret, M.; Anton, J.; Valabregue, R.; Poline, J. Region of interest analysis using an SPM toolbox. Procceedings 8th International Conference on Functional Mapping of the Human Brain; Sendai, Japan. 2002.

Bulte DP, Kelly M, Germuska M, Xie J, Chappell MA, Okell TW, Bright MG, Jezzard P. Quantitative measurement of cerebral physiology using respiratorycalibrated MRI. Neuroimage. 2012; 60:582–591. [PubMed: 22209811]

Clare S, Jezzard P. Rapid T(1) mapping using multislice echo planar imaging. Magn Reson Med. 2001; 45:630–634. [PubMed: 11283991]

Davis TL, Kwong KK, Weisskoff RM, Rosen BR. Calibrated functional MRI: mapping the dynamics of oxidative metabolism. Proc Natl Acad Sci U S A. 1998; 95:1834–1839. [PubMed: 9465103]

Fernandez-Seara MA, Edlow BL, Hoang A, Wang J, Feinberg DA, Detre JA. Minimizing acquisition time of arterial spin labeling at 3T. Magn Reson Med. 2008; 59:1467–1471. [PubMed: 18506806]

Fernandez-Seara MA, Wang Z, Wang J, Rao H, Guenther M, Feinberg DA, Detre JA. Continuous arterial spin labeling perfusion measurements using single shot 3D GRASE at 3T. Magn Reson Med. 2005; 54:1241–1247. [PubMed: 16193469]

Garcia DM, Duhamel G, Alsop DC. Efficiency of inversion pulses for background suppressed arterial spin labeling. Magn Reson Med. 2005; 54:366–372. [PubMed: 16032674]

Gauthier CJ, Hoge RD. A generalized procedure for calibrated MRI incorporating hyperoxia and hypercapnia. Hum Brain Mapp. 2013; 34:1053–1069. [PubMed: 23015481]

Ghariq E, Chappell MA, Schmid S, Teeuwisse WM, van Osch MJ. Effects of background suppression on the sensitivity of dual-echo arterial spin labeling MRI for BOLD and CBF signal changes. Neuroimage. 2014; 103:316–322. [PubMed: 25280450]

Grubb RL Jr, Raichle ME, Eichling JO, Ter-Pogossian MM. The effects of changes in PaCO2 on cerebral blood volume, blood flow, and vascular mean transit time. Stroke. 1974; 5:630–639. [PubMed: 4472361]

Gunther M, Oshio K, Feinberg DA. Single-shot 3D imaging techniques improve arterial spin labeling perfusion measurements. Magn Reson Med. 2005; 54:491–498. [PubMed: 16032686]

Jain V, Langham MC, Floyd TF, Jain G, Magland JF, Wehrli FW. Rapid magnetic resonance measurement of global cerebral metabolic rate of oxygen consumption in humans during rest and hypercapnia. J Cereb Blood Flow Metab. 2011; 31:1504–1512. [PubMed: 21505481]

Jovicich J, Norris DG. Functional MRI of the human brain with GRASE-based BOLD contrast. Magn Reson Med. 1999; 41:871–876. [PubMed: 10332867]

Kastrup A, Kruger G, Neumann-Haefelin T, Glover GH, Moseley ME. Changes of cerebral blood flow, oxygenation, and oxidative metabolism during graded motor activation. Neuroimage. 2002; 15:74–82. [PubMed: 11771975]

Keil B, Alagappan V, Mareyam A, McNab JA, Fujimoto K, Tountcheva V, Triantafyllou C, Dilks DD, Kanwisher N, Lin W, Grant PE, Wald LL. Size-optimized 32-channel brain arrays for 3 T pediatric imaging. Magn Reson Med. 2011; 66:1777–1787. [PubMed: 21656548]

Leontiev O, Buxton RB. Reproducibility of BOLD, perfusion, and CMRO2 measurements with calibrated-BOLD fMRI. Neuroimage. 2007; 35:175–184. [PubMed: 17208013]

Liu TT, Brown GG. Measurement of cerebral perfusion with arterial spin labeling: Part 1. Methods. J Int Neuropsychol Soc. 2007; 13:517–525. [PubMed: 17445301]

Liu TT, Wong EC, Frank LR, Buxton RB. Analysis and design of perfusion-based event-related fMRI experiments. Neuroimage. 2002; 16:269–282. [PubMed: 11969334]

McIntyre M, Richter W, Morden D, Wennerberg A, Frankenstein U. Blood oxygenation level dependent functional magnetic resonance imaging. Concepts Magn Reso A. 2003; 16A:5–15.

Mugler JP 3rd, Brookeman JR. Three-dimensional magnetization-prepared rapid gradient-echo imaging (3D MP RAGE). Magnetic Resonance in Medicine. 1990; 15:152–157. [PubMed: 2374495]

Norris DG, Bornert P, Reese T, Leibfritz D. On the application of ultra-fast RARE experiments. Magn Reson Med. 1992; 27:142–164. [PubMed: 1435200]

Ordidge RJ, Wylezinska M, Hugg JW, Butterworth E, Franconi F. Frequency offset corrected inversion (FOCI) pulses for use in localized spectroscopy. Magn Reson Med. 1996; 36:562–566. [PubMed: 8892208]

Rorden C, Karnath HO, Bonilha L. Improving lesion-symptom mapping. J Cogn Neurosci. 2007; 19:1081–1088. [PubMed: 17583985]

Schmithorst VJ, Hernandez-Garcia L, Vannest J, Rajagopal A, Lee G, Holland SK. Optimized simultaneous ASL and BOLD functional imaging of the whole brain. J Magn Reson Imaging. 2014; 39:1104–1117. [PubMed: 24115454]

St Lawrence KS, Frank JA, Bandettini PA, Ye FQ. Noise reduction in multi-slice arterial spin tagging imaging. Magn Reson Med. 2005; 53:735–738. [PubMed: 15723412]

Stefanovic B, Warnking JM, Rylander KM, Pike GB. The effect of global cerebral vasodilation on focal activation hemodynamics. Neuroimage. 2006; 30:726–734. [PubMed: 16337135]

Triantafyllou C, Polimeni JR, Wald LL. Physiological noise and signal-to-noise ratio in fMRI with multi-channel array coils. Neuroimage. 2011; 55:597–606. [PubMed: 21167946]

Vidorreta M, Wang Z, Rodriguez I, Pastor MA, Detre JA, Fernandez-Seara MA. Comparison of 2D and 3D single-shot ASL perfusion fMRI sequences. Neuroimage. 2013; 66:662–671. [PubMed: 23142069]

Wesolowski, R.; Gowland, PA.; Francis, ST. Proc Intl Soc Mag Reson Med. Vol. 17. Honolulu, HI: 2009. Double acquisition background suppressed (DABS) FAIR at 3T and 7T: advantages for simultaneous BOLD and CBF acquisition; p. 1526

Woolrich MW, Chiarelli P, Gallichan D, Perthen J, Liu TT. Bayesian inference of hemodynamic changes in functional arterial spin labeling data. Magn Reson Med. 2006; 56:891–906. [PubMed: 16964610]

Ye FQ, Frank JA, Weinberger DR, McLaughlin AC. Noise reduction in 3D perfusion imaging by attenuating the static signal in arterial spin tagging (ASSIST). Magn Reson Med. 2000; 44:92–100. [PubMed: 10893526]

Highlights

- An ASL dual-acquisition sequence is proposed for calibrated fMRI.
- It combines a background-suppressed 3D-GRASE readout with 2D multi-slice EPI.
- Compared to dual-echo EPI, ASL tSNR increases 3-fold without affecting BOLD tSNR.
- Fractional $CMRO_2$ changes of 12 % were measured in response to a motor task.

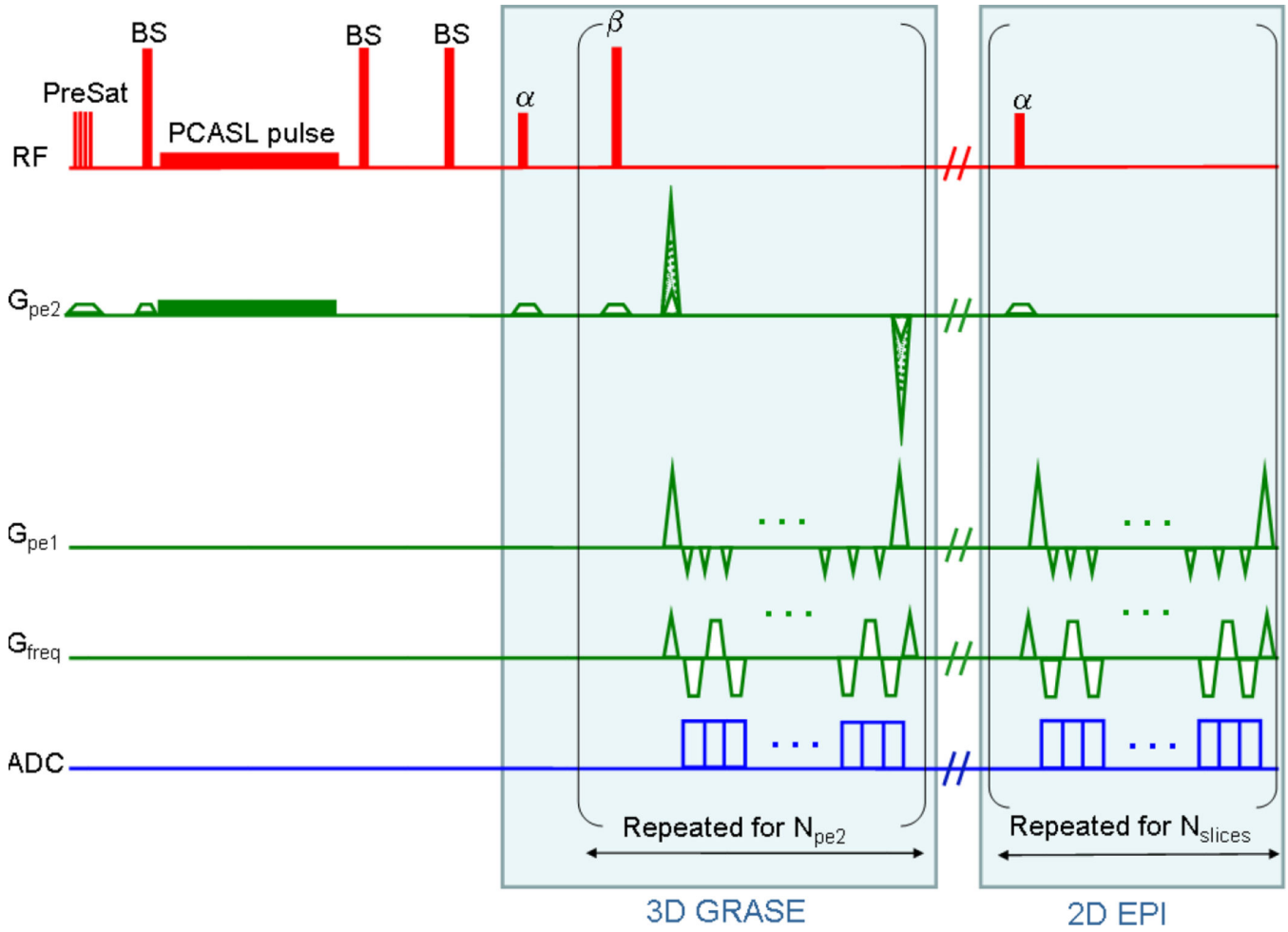

FIGURE 1.

Pulse sequence diagram showing presaturation (PreSat), background suppression (BS) and PCASL pulses, followed by the single-shot 3D-GRASE and 2D-EPI readouts, separated by a delay time of 1.3 s. The timing of the BS pulses has been optimized to null the static tissue signal at the beginning of the 3D-GRASE readout. α represents the excitation pulses and β represents the refocusing pulses. G_{pe2} refers to the second phase-encoding axis (i.e. the slice encoding axis). G_{pe1} is the first phase-encoding axis. G_{freq} is the frequency-encoding axis. N_{pe2} is the number of phase encodings in the slice encoding axis. N_{slices} is the number of slices in the 2D EPI readout.

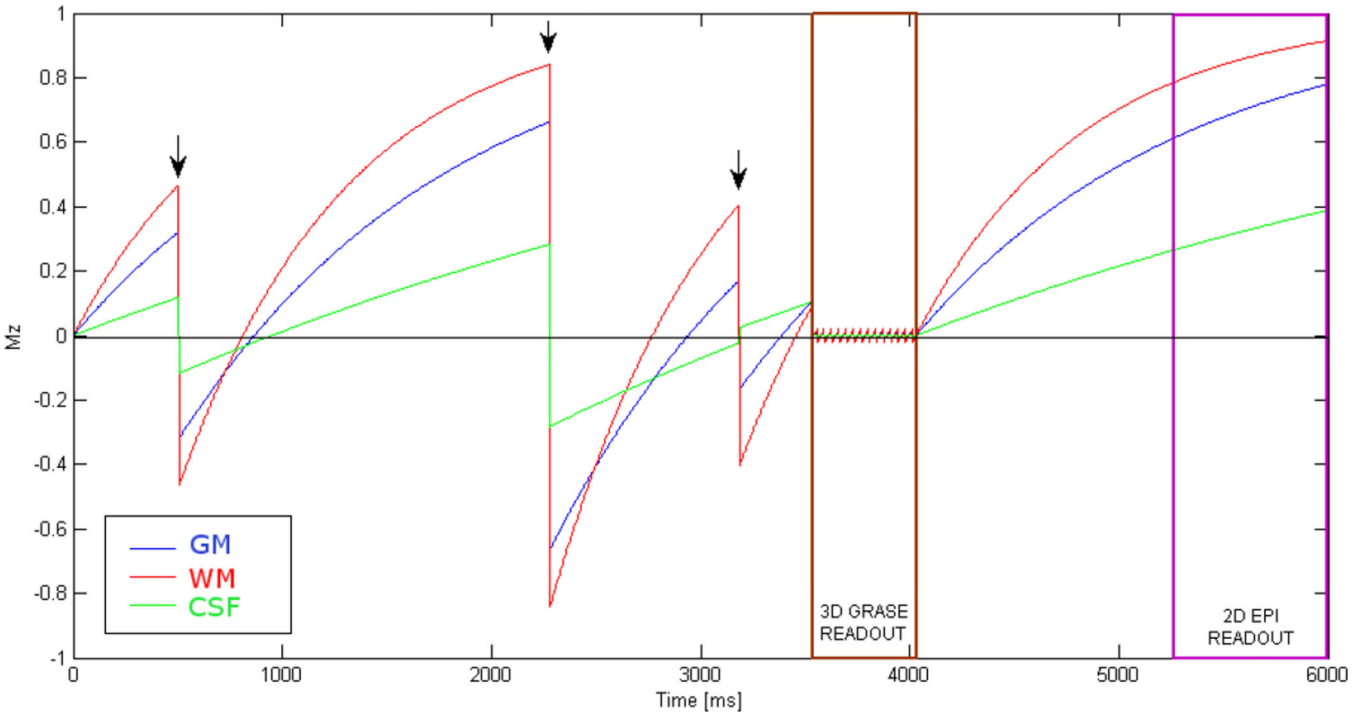

FIGURE 2.

Temporal evolution of M_z (the longitudinal component of the magnetization vector) during the dual acquisition sequence TR, for different tissue types: white matter (WM) in red, gray matter (GM) in blue and CSF in green. The timings and durations of the two readouts are indicated by the position of two rectangles (3D GRASE in brown, 2D EPI in pink). The temporal location of the BS pulses are indicated by black arrows.

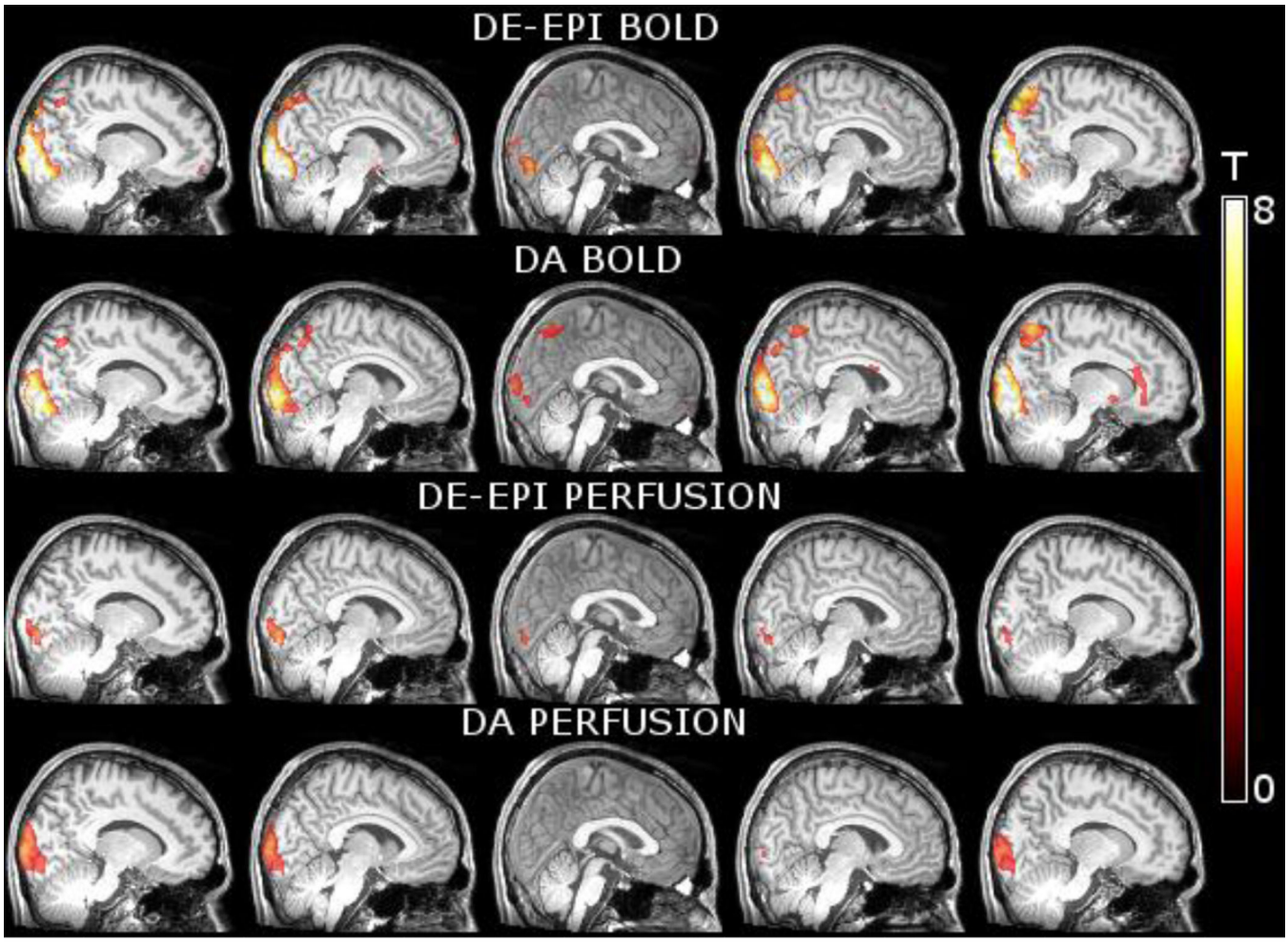

a

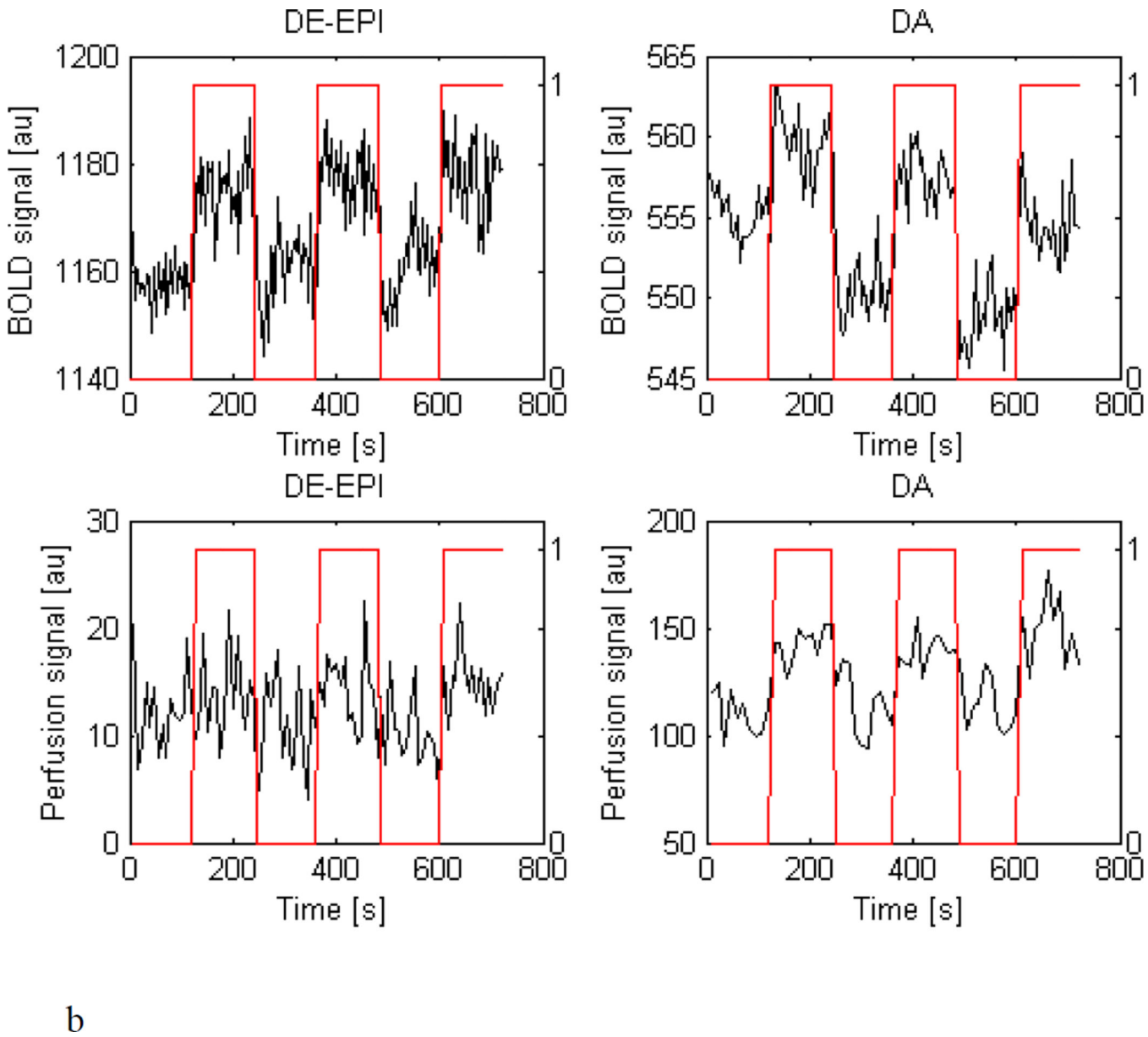

b

FIGURE 3.

(a) Areas activated by visual stimulation obtained from the four datasets acquired in a representative subject. Activation maps have been thresholded at $p<0.005$, uncorrected. (b) Signal time-courses extracted from the group maps intersection ROI (for details see methods section). The red lines represent the stimulus function.

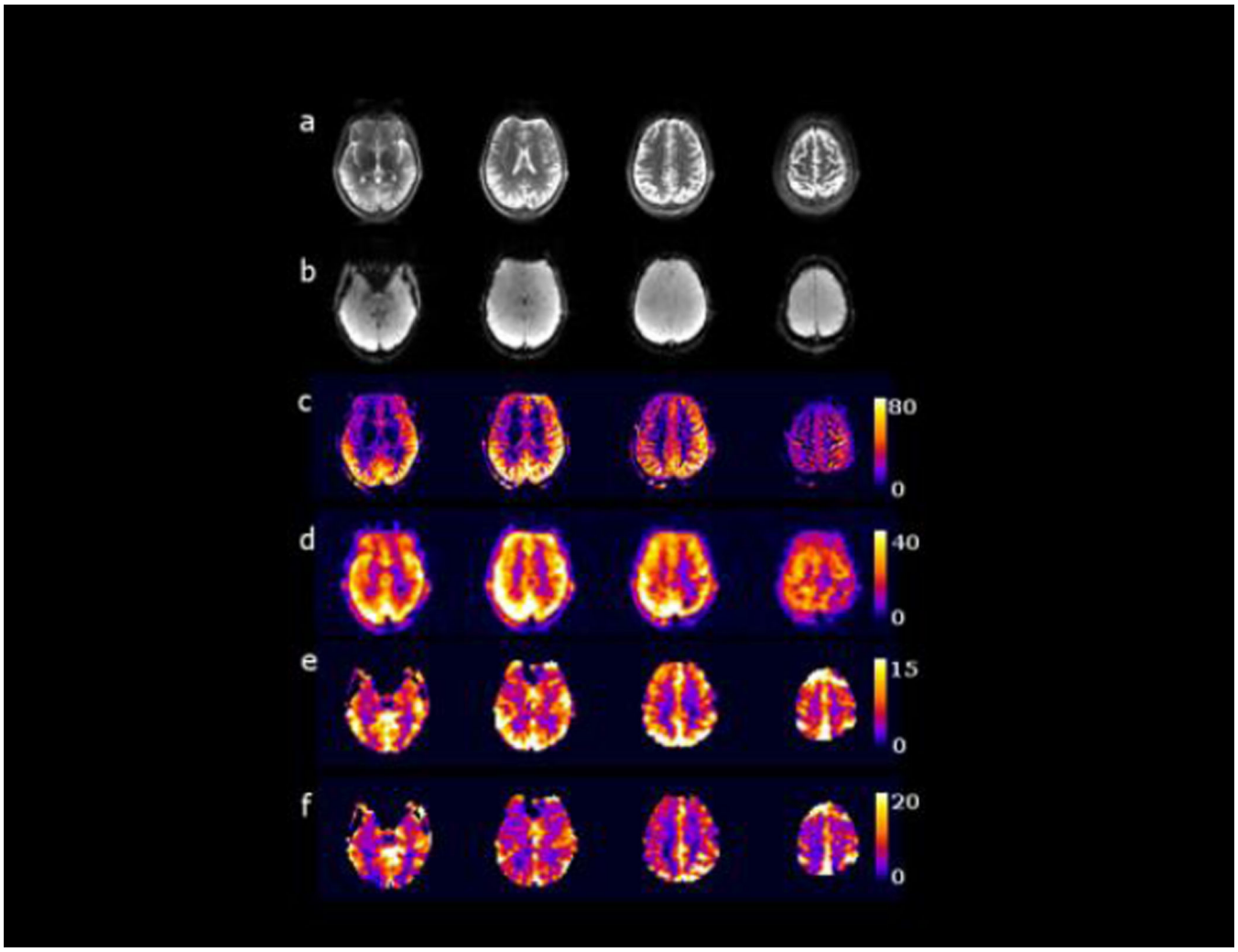

FIGURE 4.

Acquired and computed images obtained with the dual-acquisition sequence during the gas manipulation experiment in a representative subject: (a) Baseline background suppressed 3D GRASE; (b) Baseline EPI; (c) Baseline perfusion-weighted images; (d) Perfusion signal increase induced by HC; (e) BOLD signal increase induced by HC; (f) M-maps.

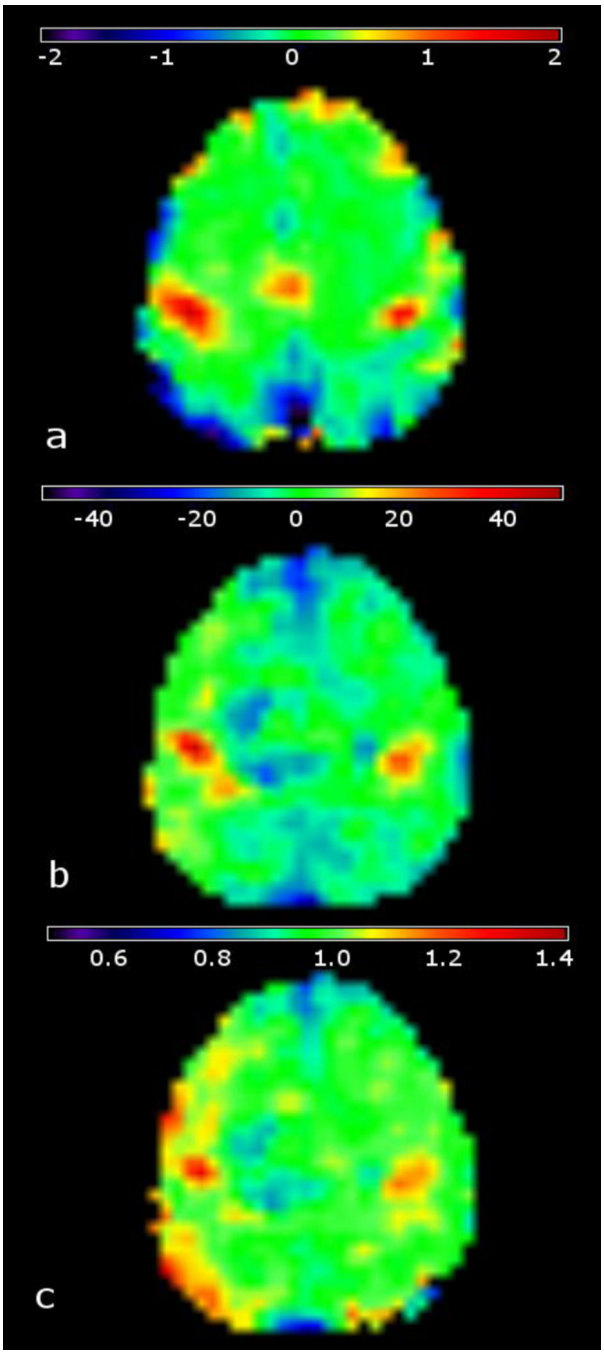

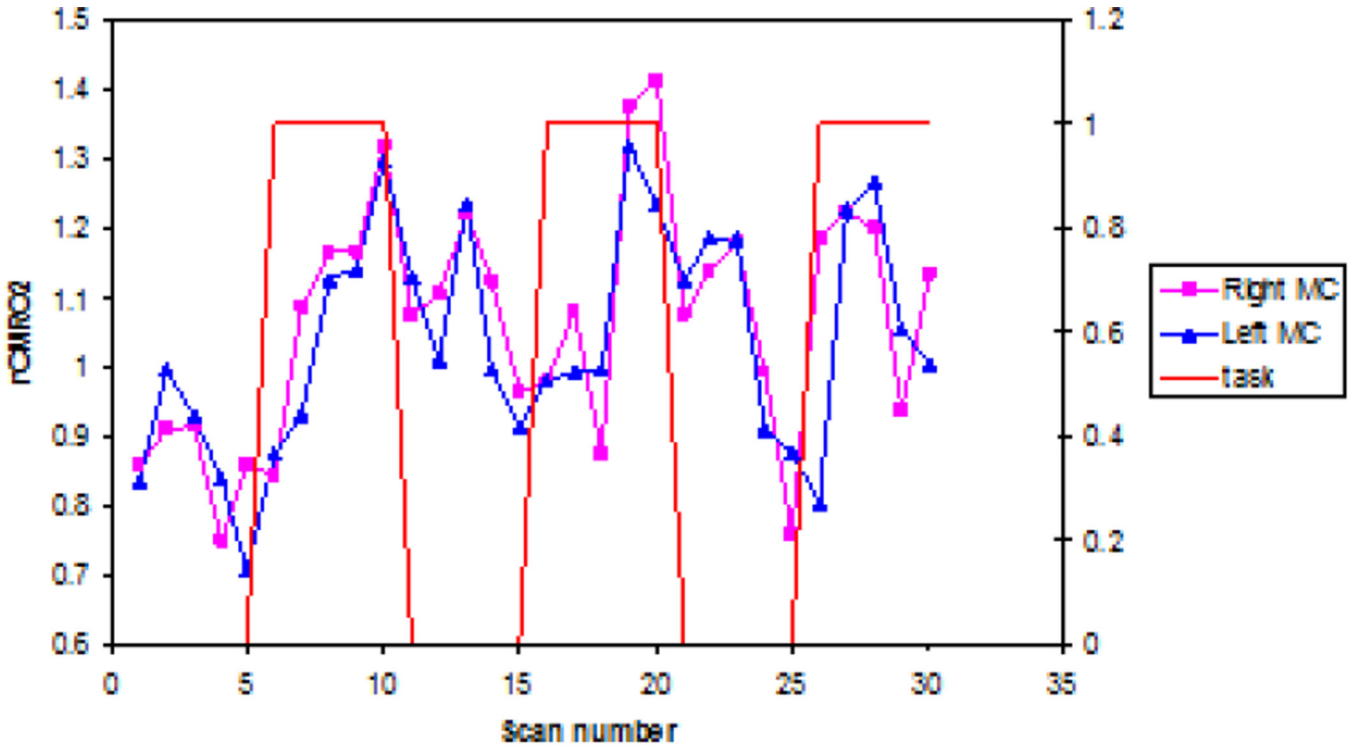

d

FIGURE 5.

Maps of signal change induced by the bilateral finger tapping task in a single subject, showing bilateral activation in the motor cortex: (a) BOLD (% of baseline); (b) Perfusion (% of baseline); (c) Relative $CMRO_2$ change during activation. (d) Relative $CMRO_2$ time courses during the fMRI paradigm computed from the BOLD and perfusion signals extracted from the activated regions in the left and right motor cortex.

Table 1

Summary of sequence parameters for the dual-echo EPI and dual-acquisition sequences

	Dual-acquisition (DA)	**Dual-echo EPI (DE-EPI)**
Number of excitations	2	1
Images per excitation	1	2
TR [s]	6	4
Spatial resolution [mm^2]	4×4	4×4
Number of slices (or partitions)	16	16
Slice thickness [mm]	6	6
ASL readout scheme	BS 3D-GRASE	Multi-slice 2D-EPI
ASL-TE	28.9 ms	10 ms
BOLD readout scheme	Multi-slice 2D-EPI	Multi-slice 2D-EPI
BOLD-TE	30 ms	30 ms
Readout duration [ms]	420 (ASL) 730 (BOLD)	812 (ASL + BOLD)
Acceleration	5/8 Partial Fourier (partition direction) (ASL)	GRAPPA-2

Table 2

a: Signal time-course parameters obtained with the four datasets. P-values refer to paired comparisons between DE-EPI and DA data.						
	BOLD			**PERFUSION**		
	DE-EPI	**DA**	**p-value**	**DE-EPI**	**DA**	**p-value**
tSNR	153.50±30.40	144.26±39.15	0.433	2.92±0.95	7.83±1.34	**7×10^{-7}**
Signal change %	1.05 ± 0.30	0.89 ± 0.30	0.134	31.32±8.50	20.43±4.52	**0.003**
CNR	1.59 ± 0.46	1.41 ± 0.69	0.380	0.90 ± 0.24	1.52 ± 0.44	**0.002**
Mean T-scores	7.70 ± 2.24	5.33 ± 1.80	**0.002**	2.25 ± 0.63	3.56 ± 1.28	**0.007**
Activated voxels (T>2.6)	9995 ± 3063	7620 ± 2857	0.039	1748±1515	5465±2835	**0.004**

b: Comparison of results obtained with the two sequences.		
	PERFUSION	**BOLD**
tSNR ratio (DA / DE-EPI)	2.94 ± 1.10	0.95 ± 0.23
Signal change ratio (DA / DE-EPI)	0.68 ± 0.19	0.89 ± 0.28
CNR ratio (DA / DE-EPI)	1.75 ± 0.53	0.91 ± 0.36
Mean T-scores ratio (DA / DE-EPI)	1.65 ± 0.52	0.73 ± 0.24
Activated voxels ratio (DA /DE-EPI)	5.68 ± 5.45	0.81 ± 0.31

DE-EPI: dual-echo EPI, DA: dual-acquisition. tSNR: temporal signal-to-noise ratio. Values are shown as mean ± standard deviation across subjects. Significant p-values after Bonferroni correction are shown in bold type.

Table 3

Calibrated fMRI results for each subject and group averages (standard deviation).

	Subject 1	Subject 2	Subject 3	Subject 4	Subject 5	Average (SD)
HC % BOLD change	3.70	3.38	3.79	3.20	3.06	3.42 (0.31)
HC % PERFUSION change	47.77	48.45	54.64	62.88	38.65	50.48 (8.98)
M (gray matter)	9.80	8.49	8.82	7.10	9.33	8.71 (1.03)
M (left MC)	8.68	9.29	8.21	3.68	6.95	7.36 (2.23)
M (right MC)	9.22	8.23	10.00	3.49	7.81	7.75 (2.53)
% BOLD change (left MC)	0.98	0.52	1.07	0.75	0.82	0.82 (0.21)
% BOLD change (right MC)	0.65	0.58	1.65	0.76	0.59	0.90 (0.51)
% PERFUSION change (right MC)	24.82	18.12	41.11	29.98	26.10	26.79 (8.20)
% PERFUSION change (left MC)	20.99	15.93	36.37	29.84	30.84	28.03 (8.47)
rCMRO2 (left MC)	1.09	1.10	1.19	1.07	1.17	1.12 (0.05)
rCMRO2 (right MC)	1.17	1.10	1.20	1.06	1.16	1.13 (0.06)

HC: hypercapnia; SD: standard deviation.